Supplementary Figure S1: Unfolded starting conformations of tRNA. (A) Unfolded coil. (B) Unfolded circle. Residues are represented by spheres and colored by index.

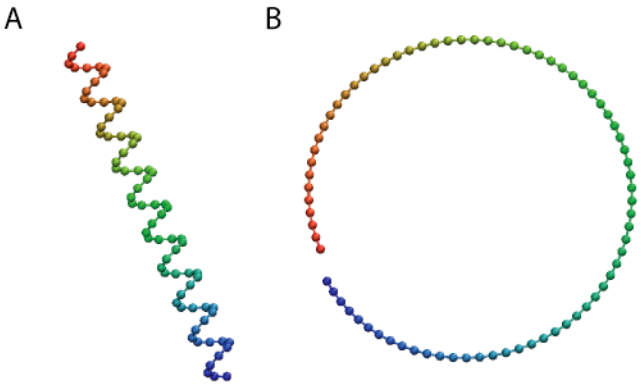

Supplementary Figure S2: Secondary structures and tertiary contacts for tRNA (A), predicted P4-P6 (B) and crystal P4-P6 (C). Segmentation definitions for tRNA and both P4-P6 secondary structures. These segments are used to reduce each molecule to the relative positions of helices, loops and junctions, which allows for faster calculations of similarities between NAST generated decoy structures.

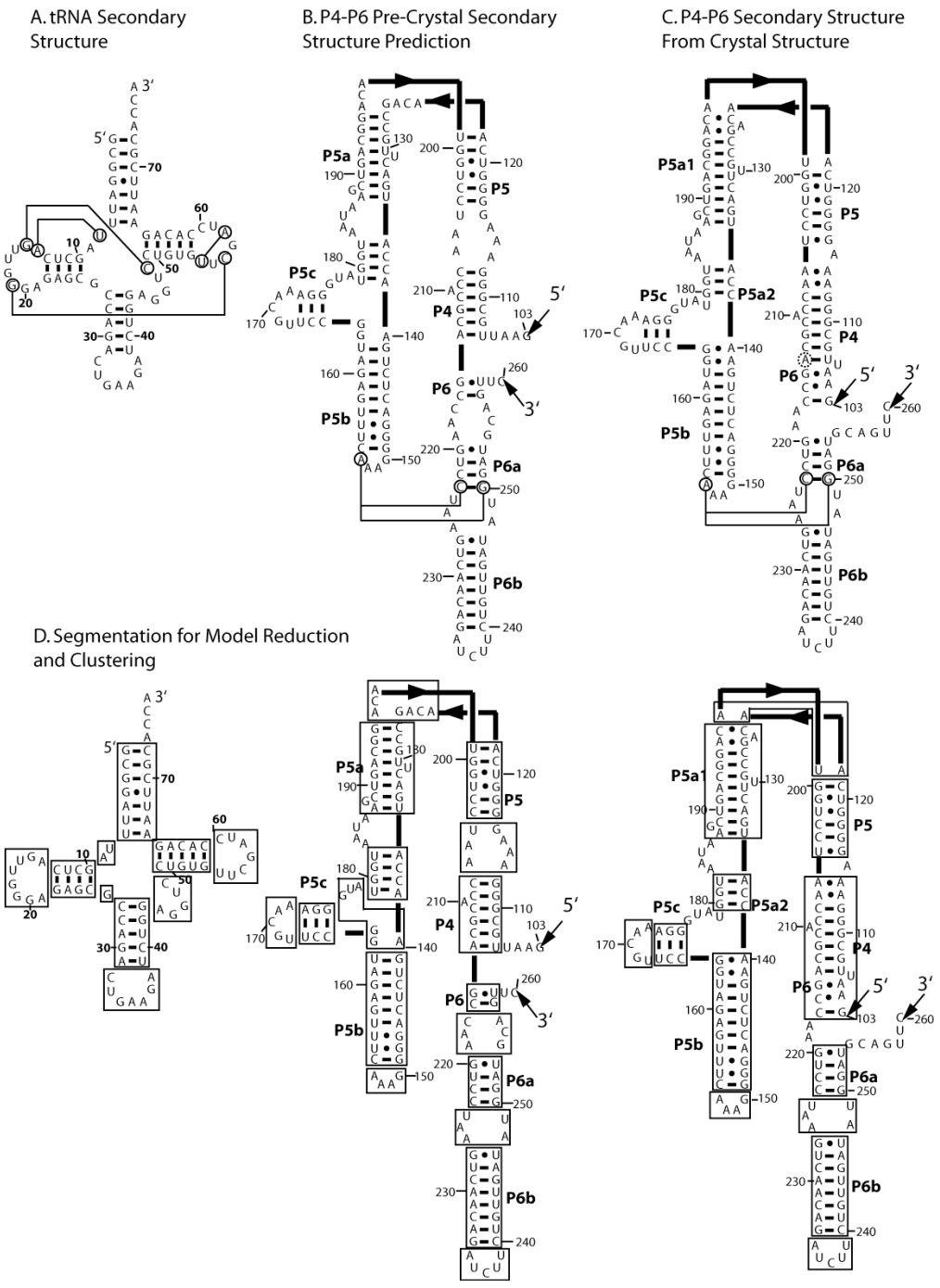

Supplementary Figure S3: Distributions of radii of gyration, GDT-TS scores and RMSD values for tRNA (A) and P4-P6 (B) structures generated using predicted (red lines) and random (green lines) tertiary contacts. We constrained both ensembles using the same secondary structure. We selected near ransom structures that matched NAST structures in their distribution of radii of gyration. For both molecules, although the distribution of radii of gyration is nearly identical, the distribution of both GDT-TS scores and RMSD values is significantly different, with the near-random compact structures scoring worse in both categories.

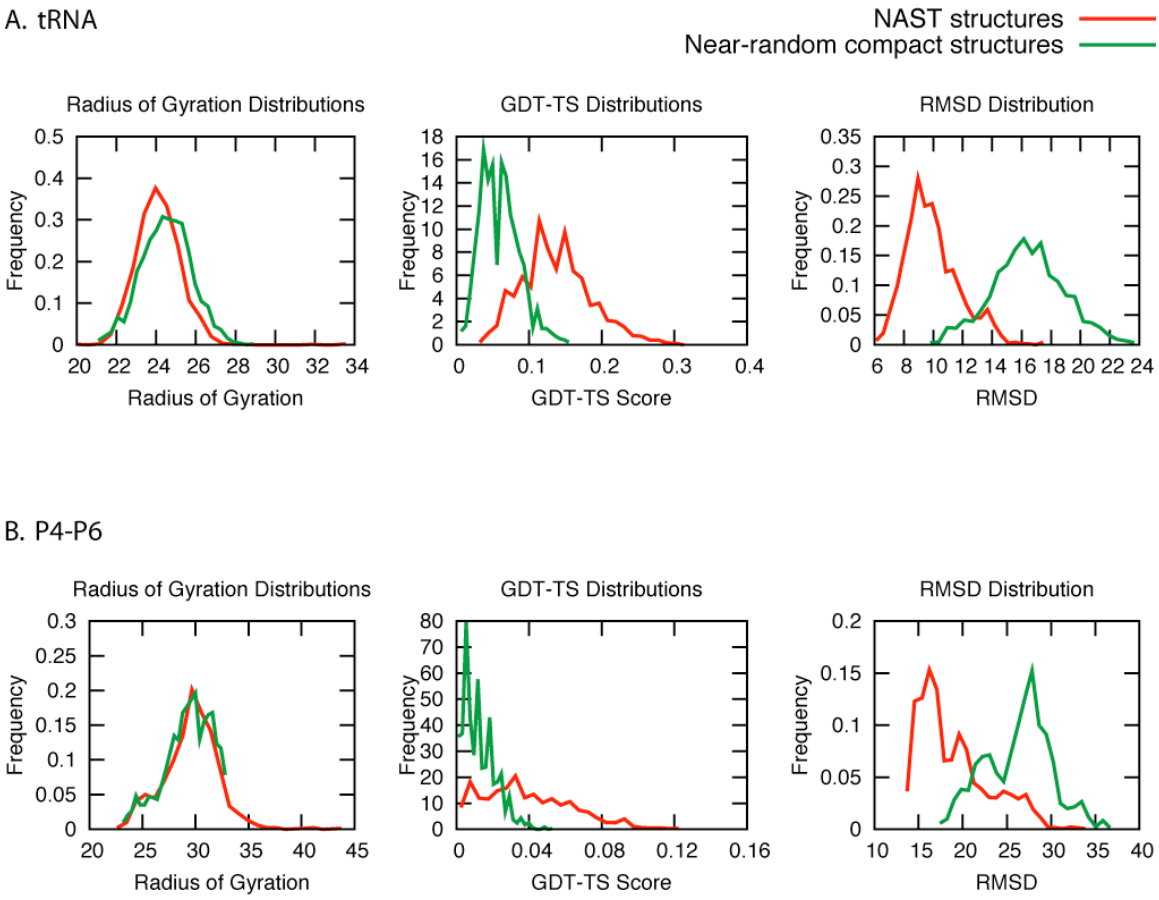

Figure S4: Ratio of within to without distances for clusters generated using k-values 1 through 5 for both tRNA (A) and P4-P6 (B). We circled the k value selected for each molecule using the elbow criterion.

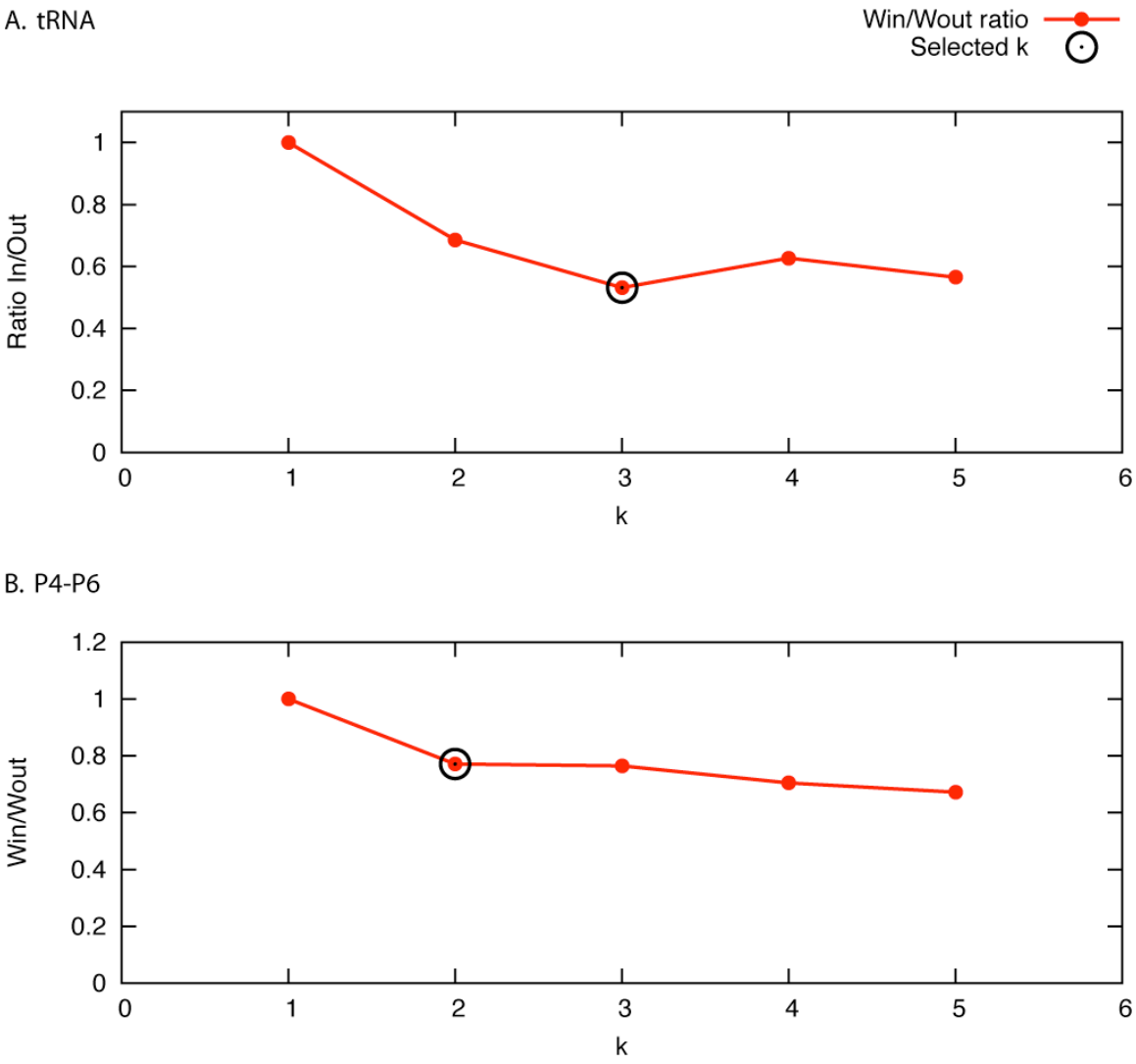

Figure S5: Relationship between GDT-TS scores and NAST energy, ideal SAXS, and ideal and experimental solvent accessibility data for tRNA. In general high GDT-TS scores correlate with low NAST energy, low error to ideal SAXS data, high correlation with both ideal and experimental solvent accessibility data.

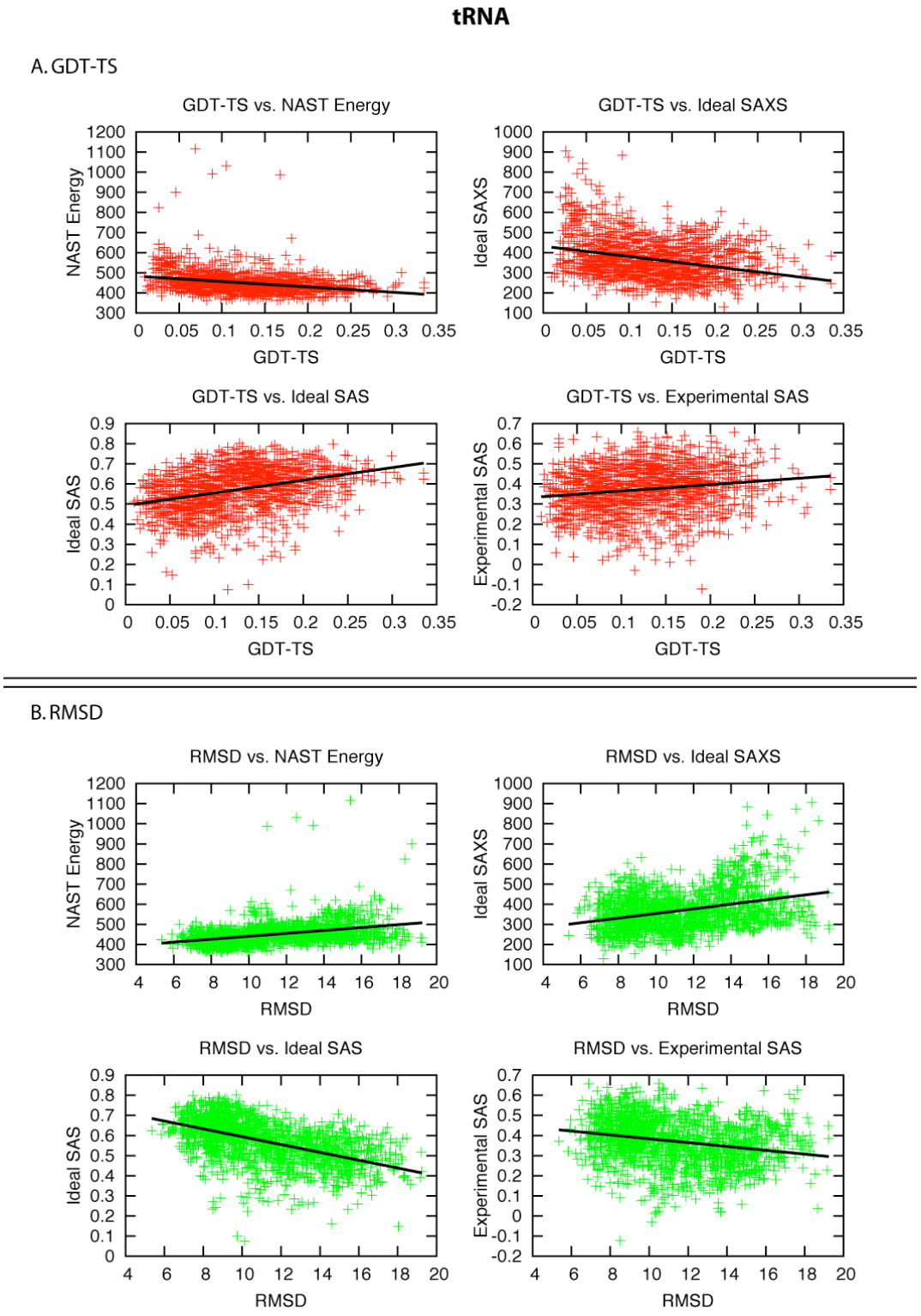

Figure S6: Relationship between GDT-TS scores and NAST energy, ideal SAXS, and ideal and experimental solvent accessibility data for P4-P6. In general high GDT-TS scores correlate with low NAST energy, low error to ideal SAXS data, high correlation with both ideal and experimental solvent accessibility data.

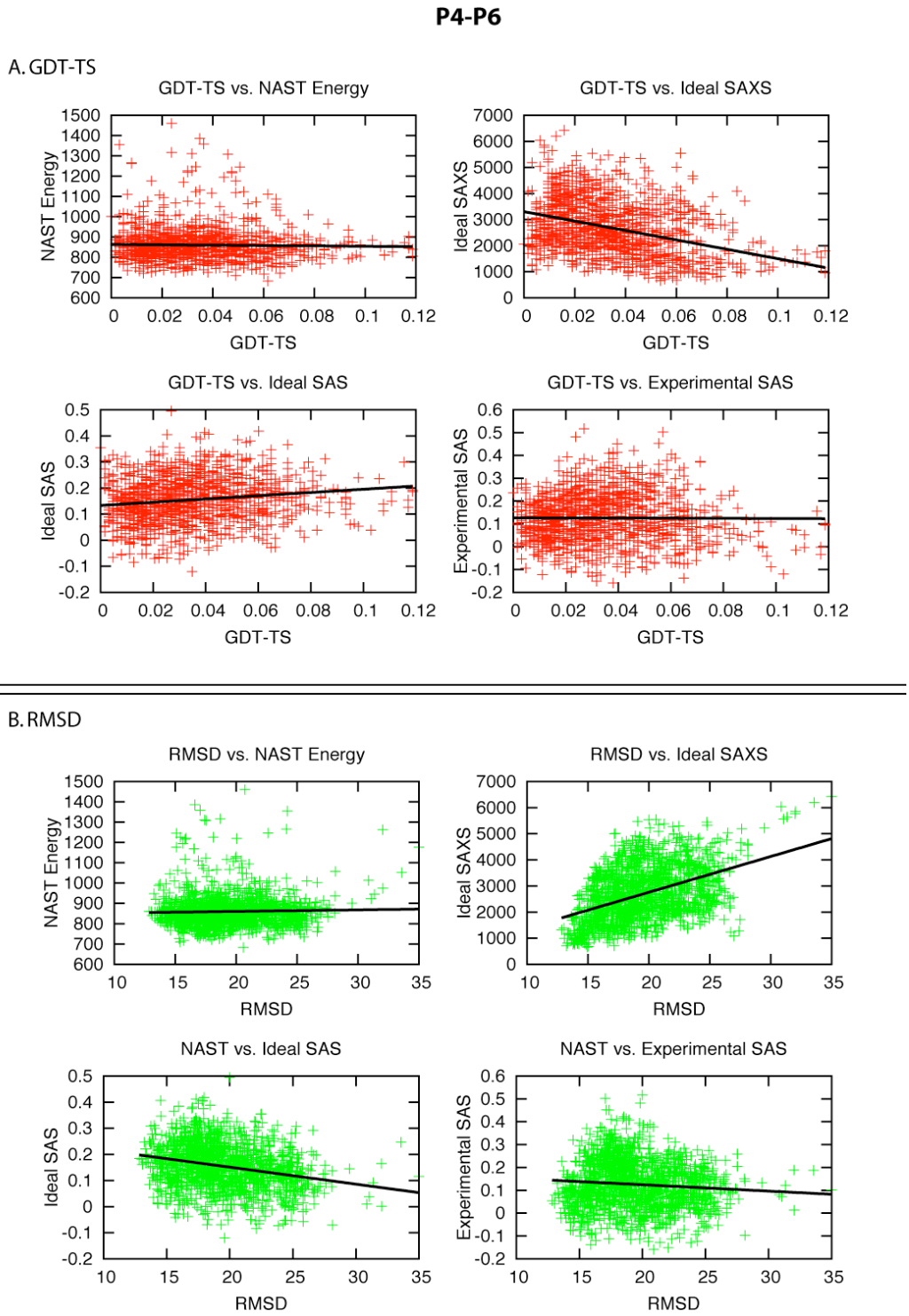

Supplementary Table S1: Parameter values for the NAST energy function.

$$U(r) = K_{PT}(r - R_{PT})^2$$

Supplementary Table S2: Average radius of gyration, GDT-TS score and RMSD values for tRNA and P4-P6 structure generated by NAST as well as near-random compact structures selected for a comparable range of radii of gyration. For similar ranges of radii of gyration, the near-random compact structures have significantly worse GDT-TS scores and RMSD values than the NAST structures.

	Near Random Compact Structures	NAST Structures
tRNA		
Radius of Gyration (Å)	24.5 ± 1.3	24.1 ± 1.1
GDT-TS Score	0.06 ± 0.03	0.14 ± 0.05
RMSD (Å)	16.4 ± 2.5	9.9 ± 1.8
P4-P6		
Radius of Gyration (Å)	29.3 ± 2.2	29.6 ± 2.6
GDT-TS Score	0.01 ± 0.01	0.04 ± 0.02
RMSD (Å)	26.3 ± 3.8	19.0 ± 4.0

Supplementary Table S3: Pearson correlation coefficients for the relationships between both GDT-TS scores and RMSD values, and NAST energy, ideal SAXS data and both ideal and experimental SAS data.

	GDT-TS	RMSD
tRNA		
NAST energy	-0.28	0.37
ideal SAXS	-0.29	0.33
ideal SAS	0.34	-0.52
exp SAS	0.16	-0.24
P4-P6		
NAST energy	-0.02	0.03
ideal SAXS	-0.36	0.45
ideal SAS	0.15	-0.26
exp SAS	-0.01	-0.09